PROCEEDINGS OF SCIENCE

Charmless B Decays at Belle II

Sagar Hazra

Tata Institute of Fundamental Research,
Mumbai 400 005, India

E-mail: sagar.hazra@tifr.res.in

We report the measurements of *CP* asymmetry and branching fraction of various charmless B decays at the Belle II experiment. We use a sample of electron-positron collisions at the $\Upsilon(4S)$ resonance that corresponds to $62.8\,\text{fb}^{-1}$ of integrated luminosity. All the results agree with previous determinations establish good performance and of the Belle II detector.

11th International Workshop on the CKM Unitarity Triangle (CKM2021)
November 22–26, 2021
The University of Melbourne, Australia

1. Introduction

The study of charmless B decays is a keystone of the flavor physics program to test the standard model (SM) and its extension. These decays are mediated by Cabbibo-suppressed $b \to u$ tree and $b \to d, s$ loop transitions, and sensitive proves to non-SM contributions. The CKM angle $\alpha/\phi_2 \equiv arg(-\frac{+_{C3}+^*_{C1}}{+_{D3}+^*_{D1}})$ can be measured directly only by an analysis of charmless $B \to \pi\pi, \rho\rho$ decays related by isospin symmetry. Isospin symmetry can be used also the make sum-rules, i.e. linear combination of branching fractions and CP asymmetries of charmless decays, that can provide test of the standard model with precision generally better than 1%. Belle II has a unique capability of studying jointly, and within a consistent experimental environment to, all relevant final states of isospin-related B decays to improve the knowledge of alpha and put stringent bound on sum-rule tests.

Belle II [2] is a magnetic spectrometer having almost 4π solid-angle coverage, designed to reconstruct final-state particles of e^+e^- collisions delivered by the SuperKEKB asymmetric-energy collider [3], located at the KEK laboratory in Tsukuba, Japan. The Belle II experiment started collecting data from March 2019. In this proceeding, we will focus on the result based on a dataset corresponding to an integrated luminosity of $62.8\,\mathrm{fb}^{-1}$ which has been collected at the $\Upsilon(4S)$ resonance.

2. Analysis overview and Challenges

We form final-state particle candidate by applying loose baseline selection criteria and then combine them in kinematic fits consistent with the topologies of the desired decays to reconstruct intermediate states and B candidates. The key challenge in reconstructing significant charmless signal is the large contamination from $e^+e^- \to q\overline{q}$ ($q = u, d, s, c$) continuum background coupled with low signal branching fraction. We use a binary-decision-tree classifier that combines a number of mostly topological variables having some discrimination between B-meson signal and continuum background. We pick up those variables whose correlation with E and M_{bc} is below ±5% to reduce possible bias in the signal yield determination. The latter two are the energy difference $E = E^* - \sqrt{s}/2$ between the energy of the reconstructed B candidate and half of the collision energy, both in the $\Upsilon(4S)$ frame, and the beam-energy-constrained mass $M_{\mathrm{bc}} = \sqrt{s/(4c^4) - (p^*/c)^2}$, which is the invariant mass of the B candidate with its energy being replaced by the half of the center-of-mass collision energy. Another challenge is to separate B background events that peak in the signal region. To deal with this peaking background, we either kinematically veto it from the sample or include a separate component in the fit model. For example, in the analysis of $B \to K\pi\pi$ decays the background from $B^+ \to \overline{D}^0(\to K^+\pi^-)\pi^+$ decays is suppressed by vetoing candidates with a kaon-pion mass in the range $[1.84, 1.89]\,\mathrm{GeV}/c^2$. We then apply optimized continuum suppression and particle identification criteria. For the signal reconstruction efficiencies calculation and fit model development, we use simulation and correct/ validate with control data. To determine the systematic uncertainties, pseudo-experiment and control channel studies are performed. We developed and tested the full analysis with simulated events and control sideband data (i.e. region where signal is not expected) before inspecting the most interesting region (or, signal region) on data to measure the physics observables.

3. Isospin sum-rule

The isospin sum-rule relation for the $B \to K\pi$ system provides a stringent test of the SM [1],

$$I_{c} = \mathcal{A}_{+c^-} + \mathcal{A}_{0c^+}\frac{\mathcal{B}(K^0\pi^+)}{\mathcal{B}(K^+\pi^-)}\frac{\tau_{0}}{\tau_{+}} - 2\mathcal{A}_{+c^0}\frac{\mathcal{B}(K^+\pi^0)}{\mathcal{B}(K^+\pi^-)}\frac{\tau_{0}}{\tau_{+}} - 2\mathcal{A}_{0c^0}\frac{\mathcal{B}(K^0\pi^0)}{\mathcal{B}(K^+\pi^-)} = 0, \quad (1)$$

where $\mathcal{B}$, $\mathcal{A}$ and τ are the branching fraction, direct CP asymmetries and lifetime of B decays, respectively. In all the four $K\pi$ channels, signal yields are determined with unbinned extended maximum-likelihood fits of the E and $M_{\rm bc}$ distributions. We measure the time-integrated asymmetry of the CP-eigenstate $B^0 \to K^0\pi^0$ by inferring the B meson flavor q from that of the other B-meson produced on the $\Upsilon(4S)$ decay, using by the category-based flavor tagger [4]. The asymmetry $\mathcal{A}_{0c^0}$ is determined from a simultaneous maximum-likelihood fit to the unbinned $M_{\rm bc}-E-q\cdot r$ distributions, where r is the dilution factor of flavor tagger output that accounts for wrongly tagged events. The signal probability density function (PDF) is given by

$$\mathcal{P}_{\rm sig} = \frac{1}{2}(1 + q(1-2w_A)\cdot(1-2\chi_3)\mathcal{A}_{0c^0}), \quad (2)$$

where χ_3 is the B^0–$\bar{B}^0$ mixing frequency. Figures 1 and 2 show the E distribution of all the four $K\pi$ system. We obtain the following branching fractions,

$$\begin{aligned}
\mathcal{B}(B^0 \to K^+\pi^-) &= [18.0 \pm 0.9(\text{stat}) \pm 0.9(\text{syst})] \times 10^{-6},\\
\mathcal{B}(B^+ \to K^+\pi^0) &= [11.9^{+1.1}_{-1.0}(\text{stat}) \pm 1.6(\text{syst})] \times 10^{-6},\\
\mathcal{B}(B^+ \to K^0\pi^+) &= [21.4^{+2.3}_{-2.2}(\text{stat}) \pm 1.6(\text{syst})] \times 10^{-6},\\
\mathcal{B}(B^0 \to K^0\pi^0) &= [8.5^{+1.7}_{-1.6}(\text{stat}) \pm 1.2(\text{syst})] \times 10^{-6}
\end{aligned}$$

and CP-violating rate asymmetries

$$\begin{aligned}
\mathcal{A}_{\%}(B^0 \to K^+\pi^-) &= -0.16 \pm 0.05(\text{stat}) \pm 0.01(\text{syst}),\\
\mathcal{A}_{\%}(B^+ \to K^+\pi^0) &= -0.09 \pm 0.09(\text{stat}) \pm 0.03(\text{syst}),\\
\mathcal{A}_{\%}(B^+ \to K^0\pi^+) &= -0.01 \pm 0.08(\text{stat}) \pm 0.05(\text{syst}),\\
\mathcal{A}_{\%}(B^0 \to K^0\pi^0) &= -0.40^{+0.46}_{-0.44}(\text{stat}) \pm 0.04(\text{syst}).
\end{aligned}$$

The dominant contribution in the systematic uncertainties comes from the π^0 and K^0_ℓ reconstruction efficiency for the decays having this final state particles. These are determined in the control sample of data and are expected to significantly reduced with larger sample size.

4. *CP* violation in multibody decays

The study of multibody charmless B decays has recently attracted significant attention [5]. The contribution between weak- and strong-interaction dynamics in $B^+ \to K^+K^-K^+$, $B^+ \to K^+\pi^-\pi^+$ and $B^0 \to K^+\pi^-\pi^0$ decays are enriched by the amplitude structure accessible via their Dalitz plot. In Fig. 3 we show the E distributions for two of these multibody systems. We obtain the following

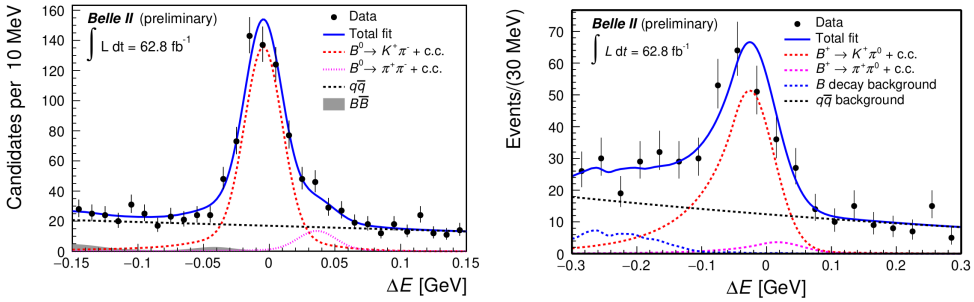

Figure 1: Signal-enhanced E distributions of $B^0 \to K^+\pi^-$ (left) and $B^+ \to K^+\pi^0$ (right).

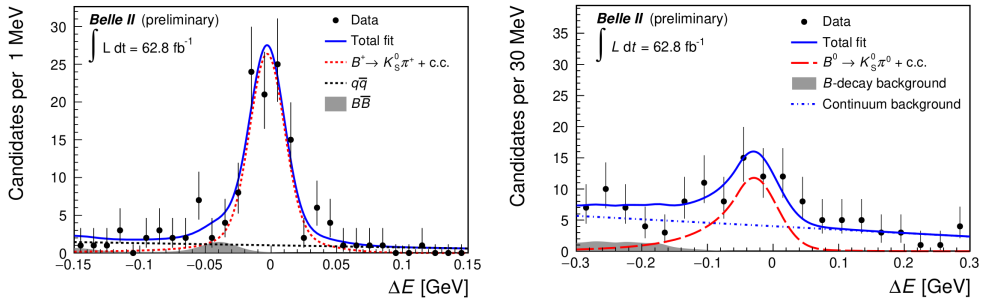

Figure 2: Signal-enhanced E distributions of $B^+ \to K^0\pi^+$ (left) and $B^0 \to K^0\pi^0$ (right).

branching fractions,

$$\begin{aligned}
\mathcal{B}(B^+ \to K^+K^-K^+) &= [35.8 \pm 1.6(\text{stat}) \pm 1.4(\text{syst})] \times 10^{-6}, \\
\mathcal{B}(B^+ \to K^+\pi^-\pi^+) &= [67.0 \pm 3.3(\text{stat}) \pm 2.3(\text{syst})] \times 10^{-6}, \\
\mathcal{B}(B^0 \to K^+\pi^-\pi^0) &= [38.1 \pm 3.5(\text{stat}) \pm 3.9(\text{syst})] \times 10^{-6}
\end{aligned}$$

and CP-violating rate asymmetries

$$\begin{aligned}
\mathcal{A}_{CP}(B^+ \to K^+K^-K^+) &= -0.103 \pm 0.042(\text{stat}) \pm 0.020(\text{syst}), \\
\mathcal{A}_{CP}(B^+ \to K^+\pi^-\pi^+) &= -0.010 \pm 0.050(\text{stat}) \pm 0.021(\text{syst}), \\
\mathcal{A}_{CP}(B^0 \to K^+\pi^-\pi^0) &= +0.207 \pm 0.088(\text{stat}) \pm 0.011(\text{syst}).
\end{aligned}$$

Also in this case, the largest systematic uncertainties comes from π^0 reconstruction for $B^0 \to K^+\pi^-\pi^0$. For the others, the dominant systematic uncertainties is the tracking efficiency, which will also be reduced with more data.

5. Towards the determination of α/ϕ_2

The combined analysis of branching fractions and CP violating asymmetries of the complete set of $B \to \pi\pi, \rho\rho$ isospin partners enables a determination of α [6]. We focus here on $B^0 \to \pi^0\pi^0$, $B^+ \to \pi^+\pi^0$, $B^0 \to \pi^+\pi^-$ and $B^+ \to \rho^+\rho^0$ decays. The $B^0 \to \pi^0\pi^0$ channel is particularly challenging as it requires the reconstruction of two $\pi^0(\to \gamma\gamma)$ decays. A dedicated boosted-decision-trees

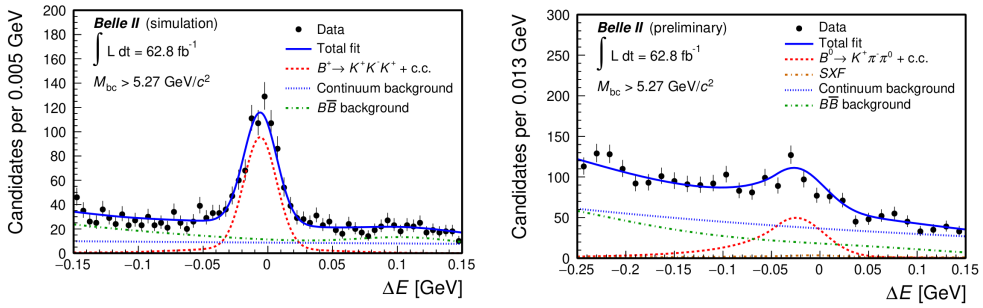

Figure 3: Signal-enhanced E distributions of $B^+ \to K^+K^-K^+$ (left) and $B^0 \to K^+\pi^-\pi^0$ (right).

classifier used to suppress background photons by combining 20 calorimetric variables. Signal yields are determined with an extended maximum-likelihood fit of the E, $M_{\rm bc}$ and transformed continuum suppression variable. Figure 4 shows the E distribution of two $\pi\pi$ channels. We obtain the following branching fractions,

$$\begin{aligned}
\mathcal{B}(B^0 \to \pi^+\pi^-) &= [5.8 \pm 0.7(\text{stat}) \pm 0.7(\text{syst})] \times 10^{-6}, \\
\mathcal{B}(B^+ \to \pi^+\pi^0) &= [5.5^{+1.0}_{-0.9}(\text{stat}) \pm 0.7(\text{syst})] \times 10^{-6}, \\
\mathcal{B}(B^0 \to \pi^0\pi^0) &= [0.98^{+0.48}_{-0.39}(\text{stat}) \pm 0.27(\text{syst})] \times 10^{-6}
\end{aligned}$$

and CP asymmetry of $\mathcal{A}_{CP}(B^+ \to \pi^+\pi^0) = -0.04 \pm 0.17(\text{stat}) \pm 0.06(\text{syst})$. The $B^+ \to \rho^+\rho^0$ decay involves pion-only final state, where the large width of the $m(\rho)$ mesons offers reduced distinctive features against dominant continuum background. Isolating a low-background signal is therefore the main challenge of the analysis. Signal yields are determined with an unbinned maximum-likelihood fits of E, continuum-suppression decision-tree output, the dipion masses and cosines of helicity angles of the ρ candidates. Figure 5 shows the E and $m(\pi^+\pi^-)$ of $B^+ \to \rho^+\rho^0$ candidates. We obtain the branching fraction $\mathcal{B} = [20.6 \pm 3.2(\text{stat}) \pm 4.0(\text{syst})] \times 10^{-6}$ and longitudinal polarization fraction $f_L = 0.936^{+0.049}_{-0.041}(\text{stat}) \pm 0.021(\text{syst})$. The dominant contribution in the systematic uncertainties comes from π^0 reconstruction and tracking efficiency.

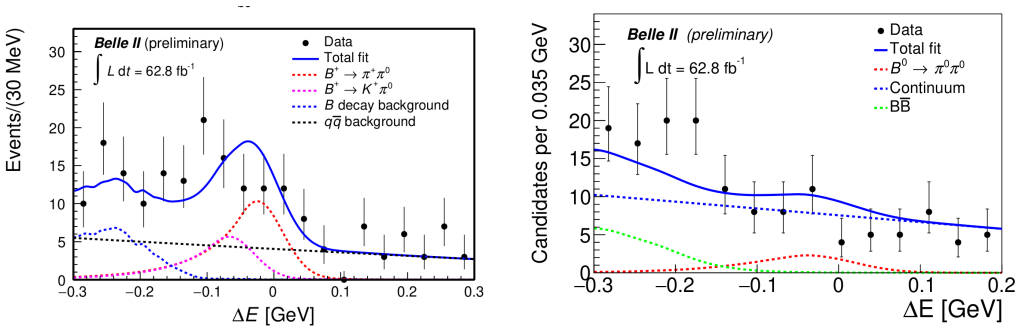

Figure 4: Signal-enhanced E distributions of $B^+ \to \pi^+\pi^0$ (left) and $B^0 \to \pi^0\pi^0$ (right).